

# Solution-processed Perovskite for Direct X-ray Detection

Chenggan Chen, Chi Li, Huan Zhang, Qing Dai\* and Hang Zhou\*, *Member, IEEE*

**Abstract**—X-ray detectors made from crystalline silicon or amorphous silicon are widely used in medical diagnosis, such as mammography or computed tomography. However, state-of-art of X-ray detectors are still suffering from high manufacturing cost. In this article, we demonstrate a methylammonium lead iodide ( $\text{CH}_3\text{NH}_3\text{PbI}_3$ ) based photodiode for direct X-ray detection. The solution-processed perovskite photodiode exhibited a good responsivity of 12.5A/W.

## I. INTRODUCTION

X-ray, discovered by W.C. Röntgen in 1895, was used in medical diagnosis and has been continuously improved with the introduction of new imaging modalities. [1][2] Currently, there are two approaches for X-ray detection, i.e. indirect conversion and direct conversion. For indirect conversion, scintillators are used to absorb X-ray to generate a large number of electrons and holes, which are trapped in the luminescence centers and recombine to produce photons in the visible wavelength. [3] For direct conversion, on the contrary, photo-conducting materials such as  $\text{PbI}_2$ , a-Se, or CdTe are directly exposed to X-ray photons and the generated carriers are collected by applying an electric field across the photoconductors. The direct detection is reported to have higher resolution, but it is difficult to deposit a homogenous film on thin film transistors which plays an important role in the readout process because of the low disintegrate temperature of the active matrix. [4-6]

Organolead halide perovskite materials have drawn great attentions in recent years, especially for photovoltaic applications. The power conversion efficiencies (PCE) of perovskite solar cells has been improved from 3.8% to above 20% in just 6 years. [7][8] Such remarkable progress is attributed to the unique properties of perovskite materials, such as long carrier diffusion lengths, high absorption characteristics, high carrier mobility and tunable optical properties.[9-11] More importantly, solution-processed perovskite is an appealing candidate for many other optoelectronic devices due to its low-temperature, non-vacuum and low cost deposition methods such as spin coating, inkjet printing, spray coating and so on. The research and development of perovskite materials in X-ray detection are also quite attractive, as it would probably lead to a new generation of low cost high resolution X-ray flat panel imager. Indeed, there are several reports on this subject. [4,12]

For direct detection of X-ray, the atomic number is usually an important parameter. Heavy atoms like Pb, Bi and Ba with large atomic numbers are ideal candidates. The excellent absorption performance of perovskite in the visible and near-IR regions and the composition of Pb and I elements have made organolead halide perovskite a competitive candidate

material for X-ray detection. Herein, we demonstrate a perovskite photodiode with the structure of ITO/PEDOT:PSS/ $\text{CH}_3\text{NH}_3\text{PbI}_3$ /PCBM/Al (Figure 1) for direct detection of X-ray photons.

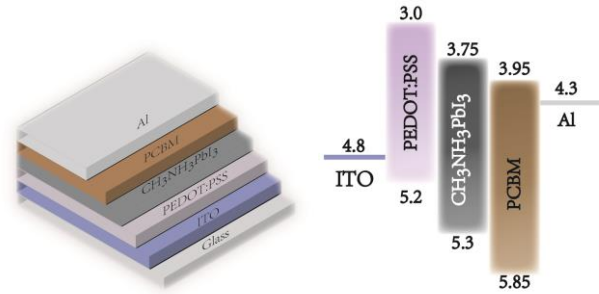


Figure 1. A typical p-i-n device configuration and schematic band diagram of the fabricated photodiode

## II. EXPERIMENTAL

### A. Materials synthesis

$\text{CH}_3\text{NH}_3\text{I}$  was synthesized by dissolving  $\text{CH}_3\text{NH}_2$  (33% in methanol, Aladdin) with  $\text{HI}$  (57% in water, Aladdin) with a volume ratio of 12:5 in a round-bottom flask, stirring in an ice bath for 2h. The solvent was removed by heating the solution in a rotary evaporator at 50°C until the white precipitate of raw  $\text{CH}_3\text{NH}_3\text{I}$  were collected. [13][14] Then the raw  $\text{CH}_3\text{NH}_3\text{I}$  was washed by ethanol, filtered and then washed by diethyl ether again. This procedure was repeated several times. Finally, the products were dried at 60 °C in a vacuum for 24h. It was then kept in the glove box for further use.

### B. Fabrication

The ITO glass substrates were cleaned by ultrasonic in abstergent, deionized water, acetone, and isopropanol for 15min each. Before the deposition process, the substrates were dried with nitrogen and treated with UV-ozone for 15min. 40nm thick hole transport layer (HTL) was formed on the cleaned ITO glass by spin-coating the PEDOT:PSS solution at 2000rpm for 40s, which was filtered through a 0.45 $\mu\text{m}$  filter. After that, the film was annealed at 150°C for 15min. After that, the substrates were moved into a glovebox to finish the following steps.  $\text{PbI}_2$  solutions were prepared by dissolving 1.2M  $\text{PbI}_2$  (99%, Aldrich) in the mixing solvent of N,N-dimethylformamide (DMF, 99.8%, Aldrich) and dimethyl sulfoxide (DMSO, 99% Aldrich). DMSO as an additive was proved to have the ability of coordinating with  $\text{PbI}_2$  by harmonize covalent bond. [15] The mixed precursor solution

Chenggan Chen, Huan Zhang and Hang Zhou (corresponding author, [Tel:+86-755-26036997](tel:+86-755-26036997), e-mail: [zhouh81@pkusz.edu.cn](mailto:zhouh81@pkusz.edu.cn)) is with the Peking University Shenzhen Graduate School, Shenzhen, 515800, China

Chi Li, Qing Dai is with the National Center for Nanoscience and Technology, 100190, China (e-mail: [daiq@nanoctr.cn](mailto:daiq@nanoctr.cn)).

was heated at 60°C for 12h under magnetic stirring before it was spin-coated on the PEDOT:PSS film at 3500, 4000, 4500, 5000rpm for 30s. Then we obtained  $\text{PbI}_2$  (DMSO)<sub>0.2</sub> complexes, which were closely packed by means of intermolecular self-assembly. Afterwards, the solution of MAI ( $\text{MA}=\text{CH}_3\text{NH}_3^+$ ) in isopropanol (30mg/ml) was dropped on the film at 5000rpm for 30s. The color of film changed from yellow to black as an intramolecular exchange of DMSO with  $\text{CH}_3\text{NH}_3\text{I}$  occurred when annealing at 150°C for 15min. In two step solution processed method, some parameters such as the ratio of DMSO and DMF in the mixing solvent, the concentration of MAI in IPA and the rotation speed of each step would be delicately adjusted to synthesize high quality perovskite films. An electron transport layer (ETL) was then deposited via spin-coating a 20mg/ml solution of PCBM in chlorobenzene, at 2000rpm for 40s. Finally, 100nm aluminum electrodes were thermally evaporated under vacuum of  $\sim 10^{-6}$  mbar, at a rate of  $\sim 3$  A/s, to complete the device.

### III. CHARACTERIZATION

For the photodiode structure, we first tested its power conversion efficiency under AM1.5 illumination. Optical absorption of the perovskite film was investigated by UV-Vis absorption spectra. A field-emission scanning electron microscope (Hitachi S-4800) was used to investigate the surface morphology of the perovskite. The fabricated photodiode was subjected to a home-made X-ray source for X-ray detect studies. Our X-ray source was generated by the bombardment of Mo target with the electron generated from field emission of carbon nanotube arrays. (Figure2)

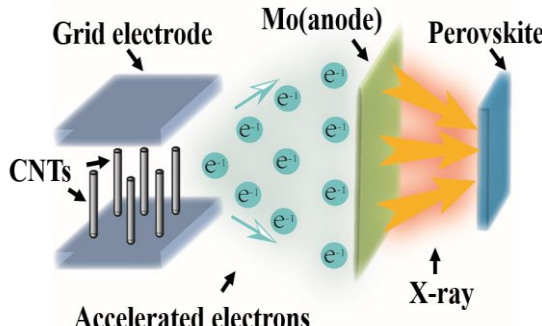


Figure 2. Schematic drawing of the experimental setup

### IV. RESULTS AND DISCUSSION

As shown in Figure3 the photovoltaic device provided a power conversion efficiency of 10.46%. In conventional process,  $\text{PbI}_2$  films were annealed at high temperature to achieve good interdiffusion. But a compact layer of  $\text{PbI}_2$  was not appropriate to react with MAI solution. Here we deposited the  $\text{PbI}_2$  without additional annealing process. When MAI solution drop on the pre-formed  $\text{PbI}_2$ , an exchange of MAI and DMSO molecules occurred, which lead to a considerable

uniform perovskite film. Figure4 shows the  $\text{CH}_3\text{NH}_3\text{PbI}_3$  with large grainsize and perfect crystallization.

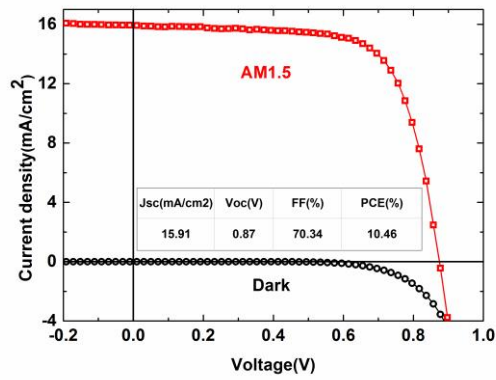


Figure 3. J-V curve of the perovskite solar cell under darkness and AM1.5G conditions

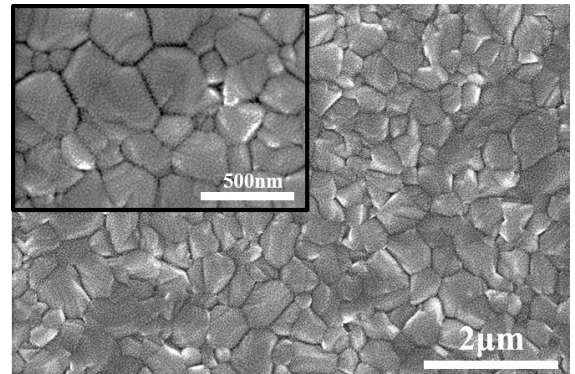


Figure 4. Top view scanning electron microscopy (SEM) images

The perovskite film showed an absorption edge at 770 nm, agreeing with the bandgap of  $\text{CH}_3\text{NH}_3\text{PbI}_3$  (1.55eV). Little change was found in the absorption spectrum with the different rotation speed of  $\text{PbI}_2$ . We observed a small absorption edge at about 550nm, which is related to the bandgap of  $\text{PbI}_2$ . This phenomenon indicated that the fabricated perovskite films had  $\text{PbI}_2$  remained, which was beneficial to the absorption of X-ray. (Figure 5)

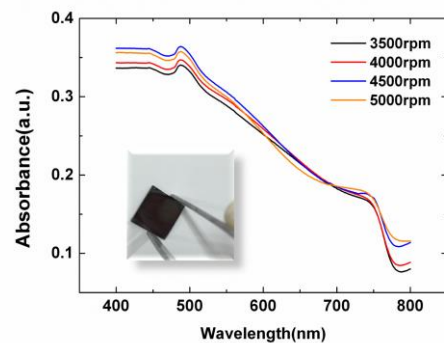
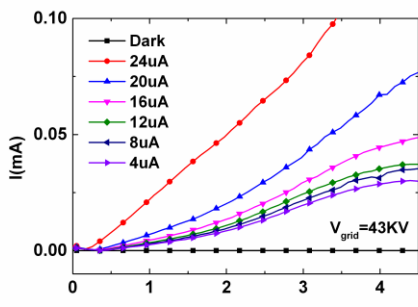
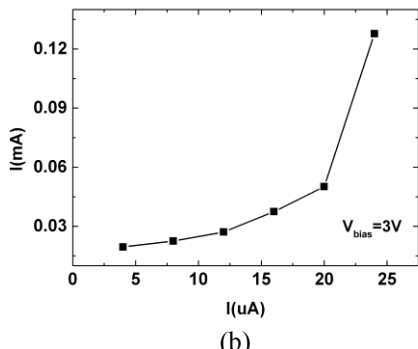


Figure 5. Absorption of the perovskite films with varied rotation speed of  $\text{PbI}_2$ . The inset shows the picture of the perovskite films



(a)



(b)

Figure 6. (a) Photon current vs bias voltage of the photodiode when the anode current of X-ray source varied from  $4\mu\text{A}$  to  $24\mu\text{A}$ , grid voltage was  $43\text{kV}$ . (b) Photon current vs anode current at a focused bias voltage of  $3\text{V}$

With no X-ray irradiation, we have obtained a dark current of  $2\text{nA}$ , which magnified to about  $25\text{nA}$  when exposed to the X-ray. The calculated responsivity was  $12.5\text{ A/W}$ .

$$R = \frac{I}{P} = \frac{I_p/S}{U \cdot I_{anode}}$$

where  $I_p$  is the photocurrent,  $S$  is the active area of the photodetector,  $U$  is the anode voltage ( $45\text{kV}$ ) and  $I_{anode}$  is the anode current. As we changed the anode current and the bias across the device, we observed obvious photocurrent generation. (Figure 6) Under high bias voltage about  $4\text{V}$  the photocurrent is approach to saturation when anode current is low. But at a high anode current the photocurrent still increases with the increasing bias voltage. This phenomenon shows that our photodetector is highly sensitive to X-rays. Compared to the previous reporting, our perovskite exhibited excellent both in solar cell and photodetector.

X-ray has energy range from  $10\text{k-1M eV}$  ( $E = 10.8 \times Z^2$ , where  $Z$  is the atomic number), for Mo,  $Z=42$ , and  $E=19\text{keV}$ . At such high photon energy, the absorption length in perovskite materials can be  $10\text{-}100\text{ um}$ , which is more than two orders of magnitude larger than its absorption length in the visible light.[4] The thickness of our perovskite layer was only  $200\text{-}300\text{nm}$  when using the spin-coating method. It is expected that if we could increase the thickness of the device,

the responsivity of the perovskite photodiode detector would be higher.

Common X-ray detector based on silicon or selenium materials inevitably adopted high vacuum deposition methods and their manufacturing processes require several photolithography steps, which raises the cost of the final products. For perovskite photodetector, the whole fabrication process could be done in low temperature at an ambient environment, which were key factors for low cost production. What's more, the organolead halide perovskites could be used to make flexible device which may find potential new applications in medical area.

## V. CONCLUSION

High quality  $\text{CH}_3\text{NH}_3\text{PbI}_3$  and corresponding photodiode were prepared by an intramolecular exchange two-step solution process. The device performed high power conversion efficiency of up to  $10\%$ . For the detection of X-ray, we observed obvious photocurrent generation from  $2\text{nA}$  to  $25\text{nA}$  when the photodiode exposed to X-ray source and the responsivity was above  $12\text{ A/W}$ .

## ACKNOWLEDGMENT

This research was supported by Shenzhen Science and Technology Foundation (KQCX20140522143114399), National Natural Science Foundation Projects (11427808), and the “Strategic Priority Research Program” of the Chinese Academy of Sciences (Grant No. XDA0909040200).

## REFERENCES

- [1] M. Spahn, “X-ray detectors in medical imaging,” Nuclear Instruments and Methods in Physics Research A, vol. 731 pp. 57–63, 2013.
- [2] I. Sechopoulos, “A review of breast tomosynthesis. Part I. The image acquisition process,” Medical Physics, vol. 40, No. 1, 2013.
- [3] M. Nikl, “Scintillation detectors for x-rays,” Measurement Science and Technology, vol. 17, R37–R54, 2006.
- [4] S. Yakunin, “Detection of X-ray photons by solution-processed lead halide perovskites” Nature Photonics, vol.9, pp. 444-450, 2015.
- [5] Kasap, S. O. & Rowlands, J. A. “Direct-conversion flat-panel X-ray image sensors for digital radiography,” Proc. IEEE, vol. 90, pp. 591 – 604, 2002.
- [6] Kasap, S. et al. “Amorphous and polycrystalline photoconductors for direct conversion flat panel X-ray image sensors,” Sensors, vol. 11, pp. 5112 –5157, 2011.
- [7] A. Kojima, K. Teshima, Y. Shirai, T. Miyasaka, “Organometal Halide Perovskites as Visible-Light Sensitizers for Photovoltaic Cells” Journal of the American Chemical Society. Vol. 131, pp. 6050-6051, 2009.
- [8] Yang, W. Seok, et al. “High-performance photovoltaic perovskite layers fabricated through intramolecular exchange” Science, Vol. 348, Issue 6240, pp.1234-1237, 2015.
- [9] S. Stranks, G. Eperon, G. Grancini, C. Menelaou, M. Alcocer, T. Leijtens, L. Herz, A. Petrozza, and H. Snaith, “Electron-Hole Diffusion Lengths Exceeding 1 Micrometer in an Organometal Trihalide Perovskite Absorber,” Science, vol. 342, Issue. 6156, pp. 341–344, 2013.

- [10] C. Wehrenfennig, G. Eperon, M. Johnston, H. Snaith, and L. Herz, “High Charge Carrier Mobilities and Lifetimes in Organolead Trihalide Perovskites,” *Advanced materials*, vol. 26, No. 10, pp. 1584–1589, 2014.
- [11] J. Noh, S. Im, J. Heo, T. Mandal, and S. Seok, “Chemical Management for Colorful, Efficient, and Stable Inorganic–Organic Hybrid Nanostructured Solar Cells,” *Nano Letters*, vol. 13, pp. 1764–1769, 2013.
- [12] H. Wei, Y. Fang, P. Mulligan, W. Chuirazzi, H. Fang, C. Wang, B. Ecker, Y. Gao, M. Loi, L. Cao & J. s. Huang, “Sensitive X-ray detectors made of methylammonium lead tribromide perovskite single crystals” *Nature Photonics* vol.10, pp.333–339, 2016
- [13] H. S. Kim, C. R. Lee, J. H. Im, K. B. Lee, T. Moehl, A. Marchioro, S. J. Moon, R. H. Baker, J.H. Yum, J. E. Moser, M. Gr'atzel and N. G. Park, “Lead Iodide Perovskite Sensitized All-Solid-State Submicron Thin Film Mesoscopic Solar Cell with Efficiency Exceeding 9%” *Scientific reports*, vol. 2, pp. 591, 2012.
- [14] J. H. Im, C. R. Lee, J. W. Lee, S. W. Park and N. G. Park, “6.5% efficient perovskite quantum-dot-sensitized solar cell” *Nanoscale*, vol. 3, pp. 4088–4093, 2011.
- [15] W. Li, J. Fan, J. Li, Y. Mai, L. Wang, “Controllable Grain Morphology of Perovskite Absorber Film by Molecular Self-Assembly toward Efficient Solar Cell Exceeding 17%” *Journal of the American Chemical Society, Soc.* Vol. 137, pp. 32, 2015.